Rev.Adv.Mater.Sci. 15(2007) 225-233

ELECTROCATALYSIS AND BIOELECTROCATALYSIS AT NANOSTRUCTURED COMPOSITE FILMS

P. J. Kulesza[1], R. Marassi[2], K. Karnicka[1], R. Wlodarczyk[2,3], K. Miecznikowski[1], M. Skunik[1], B. Kowalewska[1], M. Chojak[1], B. Baranowska[1], A. Kolary-Zurowska[1,2] and G. Ginalska[4]

[1]Department of Chemistry, University of Warsaw, Pasteura 1, PL-02-093 Warsaw, Poland
[2]Department of Chemistry, University of Camerino, S. Agostino 1, I-62032 Camerino, Italy
[3]Division of Chemistry, Department of Materials and Process Engineering and Applied Physics, Czestochowa University of Technology, Al. Armii Krajowej 16, PL 42-200 Czestochowa, Poland
[4]Division of Biochemistry, Medical Academy, PL-20-093 Lublin, Poland

Received: January 22, 2007

Abstract. The modification of Pt nanoparticles by adsorbing monolayers of phosphododecatungstic acid on their surfaces tends to activate them towards efficient electrocatalytic reduction of oxygen in acid medium. The modification steps were performed either before or after introduction of Pt nanoparticles onto the glassy carbon substrates. Formation of a stable colloidal suspension of phosphotungstate protected Pt-nanoparticles was required in the first case; whereas, in the second case, bare Pt nanoparticles had been deposited on glassy carbon before they were subsequently modified with $H_3PW_{12}O_{40}$. Rotating disk voltammetry was used to probe the electroreduction of dioxygen in 0.5 mol dm^{-3} H_2SO_4 at 25 °C. $H_3PW_{12}O_{40}$ could act as both effective mediator (e.g. for the reduction of the hydrogen peroxide intermediate) and the source of mobile protons at the electrocatalytic interface. The above concept of bifunctional catalytic system has been extended to the bioelectrocatalytic reduction of oxygen in neutral medium (0.1 mol dm^{-3} KCl) at the electrode modified with multi-walled carbon nanotube supported Co-protoporphyrin/horseradish peroxidase hybrid (composite) bioinorganic catalyst.

1. INTRODUCTION

The ability of Keggin type polyoxometallates to exhibit fast reversible multi-electron transfers prompted interest in the systems as electrocatalysts for various inert redox reactions including hydrogen evolution and oxygen reduction [1-6]. It has been recognized that the partially reduced heteropolyanions of W and Mo (heteropolyblues) provide highly reactive mixed-valence redox centers. In principle, heteropolytungstates and molybdates can be used in electrocatalysis as homogeneously dissolved species or, preferably, as materials persistently attached to electrode surfaces [2-4]. Different approaches to immobilization of POMs on electrode surfaces have been proposed. They include electrodeposition [5,6], controlled fabrication of multi-layered structures by alternate immersions in the appropriate solutions of heteropolyanion and cationic (organic or inorganic) species [7], immobilization in conductive polymer matrices [8] or ion exchange polymer films [9], as well as simple attachment by adsorption on the activated carbon substrates [10].

Corresponding author: P. J. Kulesza, e-mail: pkulesza@alfa.chem.uw.edu.pl

Efficient electrocatalytic systems for oxygen reduction or hydrogen oxidation, in which loading of the noble metal catalyst is reduced, would utilize highly-dispersed large-surface area nanosized Pt crystallites [11]. In the first approach to activate Pt nanoparticles with PW_{12} pursued in the present work, initial immobilization of small amounts of spherical Pt nanoparticles on the inert glassy carbon substrate has been followed by modification of their surfaces with ultra-thin films of Keggin type heteropolyacids of molybdenum or tungsten. Our goal has been to combine the powerful electrocatalytic properties of platinum [12-14] with the fast electron transfer capabilities, proton mobility and high reductive reactivity of Keggin type $H_3PW_{12}O_{40}$ (PW_{12}). By analogy to parent tungsten oxides, the related polytungstate is expected to interact strongly with platinum particles and to enhance their electrocatalytic reactivity towards the reduction of oxygen [6] and the oxidation of methanol [15]. To prepare ultra-thin films of nanostructured PW_{12}, we have explored the fact that heteropolyanion tends undergo strong adsorption on platinum and carbon substrates [16]. In particular, Pt nanoparticles can be stabilized by modifying their surfaces with robust anionic polyoxometallate monolayers [17]. The adsorptive interactions are strong enough to permit formation of stable colloidal solutions of polyoxometallate-protected Pt-nanoparticles [16,17] or carbon nanostructures [18]. Therefore, our second approach utilized PW_{12}- stabilized (and simultaneously activated) Pt-nanoparticles from the colloidal solutions mentioned above.

The above concepts are, however, of limited use for electrocatalytic reduction of oxygen in biological media of neutral pH. Under such conditions, the reduction of oxygen proceeds at platinum electrocatalysts as a two-step reaction via sizeable production of hydrogen peroxide intermediate. Further, platinum is likely to undergo poisoning by various organic species. Therefore, we propose a composite film that utilizes carbon nanotubes as conductive supports of high surface area codeposited together with a bifunctional electrocatalytic system composed of Co-porphyrin and the enzyme (horseradish peroxidase) are immobilized. While the Co-porphyrin centers tend to induce reduction of oxygen at the initial stage, the enzyme acts as highly reactive electrocatalyst for undesirable hydrogen peroxide intermediate. Consequently, an effective electrocatalytic film for reduction of oxygen (predominantly to water as a final product) under neutral conditions is produced. This research is of importance to the development of so called biofuel cells. Typical redox processes considered for biofuel cells involve the anodic oxidation of fuels such as glucose or ethyl alcohol combined with the reduction of oxygen at the cathode. Optimization of the latter process in terms of discovering highly efficient biocatalyst with long-term stability seems to be crucial for the further development of biofuel cells. So far, the most commonly considered biocatalytic enzymes for the cathodic side in biofuel cells are laccase and bilirubin oxidase (BOD) [19-25]. In this context, a classic, fairly cheap and robust enzyme such as horseradish peroxidase (combined with macromolecular metalloporphirine) could be an interesting alternative.

2. EXPERIMENTAL

All chemicals were commercial materials of analytical grade purity and were used without further purification. Platinum black clusters (surface area, 20 $m^2\ g^{-1}$) were obtained from Johnson & Matthew. Solutions were prepared using doubly-distilled and subsequently de-ionized (Millipore Milli-Q) water. To produce a suspension of bare platinum nanoparticles (~ 8 nm diameter), a known amount (0.1 g) of platinum black dispersed in 8 cm^3 of water was used. The suspension was sonicated for ca. 48 h. PW_{12}-protected platinum nanoparticles (PW_{12}-Pt) were produced as follows. A suspension of a known amount (0.33 g) of Pt black was formed in 10 mmol dm^{-3} aqueous PW_{12} solution (10 cm^3). The suspension was sonicated for 2 h, left overnight and then centrifuged 3-4 times. Each supernatant solution was removed and replaced with a fresh PW_{12} solution. The final centrifuging step was done with water. The resulting Pt-PW_{12} colloidal suspension (pH ≈ 3) was stable for at least a month.

Glassy carbon (GC) disk (geometric surface area, 0.071 cm^2) served as a working electrode. Argon was used to de-aerate solutions and to keep air-free atmosphere over the solution during the measurements. All experiments were performed at room temperature (25 °C).

Before modification, glassy carbon disks (geometric area, 0.071 cm^2) were activated by polishing with successively finer grade aqueous alumina slurries (grain size, 5-0.5 mm) on a Buehler polishing cloth. To immobilize bare Pt nanoparticles on glassy carbon, 1 μdm^3 aliquot of Pt suspension was placed on its surface with the use of micropipette and left 15 min to dry at room temperature. To assure homogeneous and firm attachment, the elec-

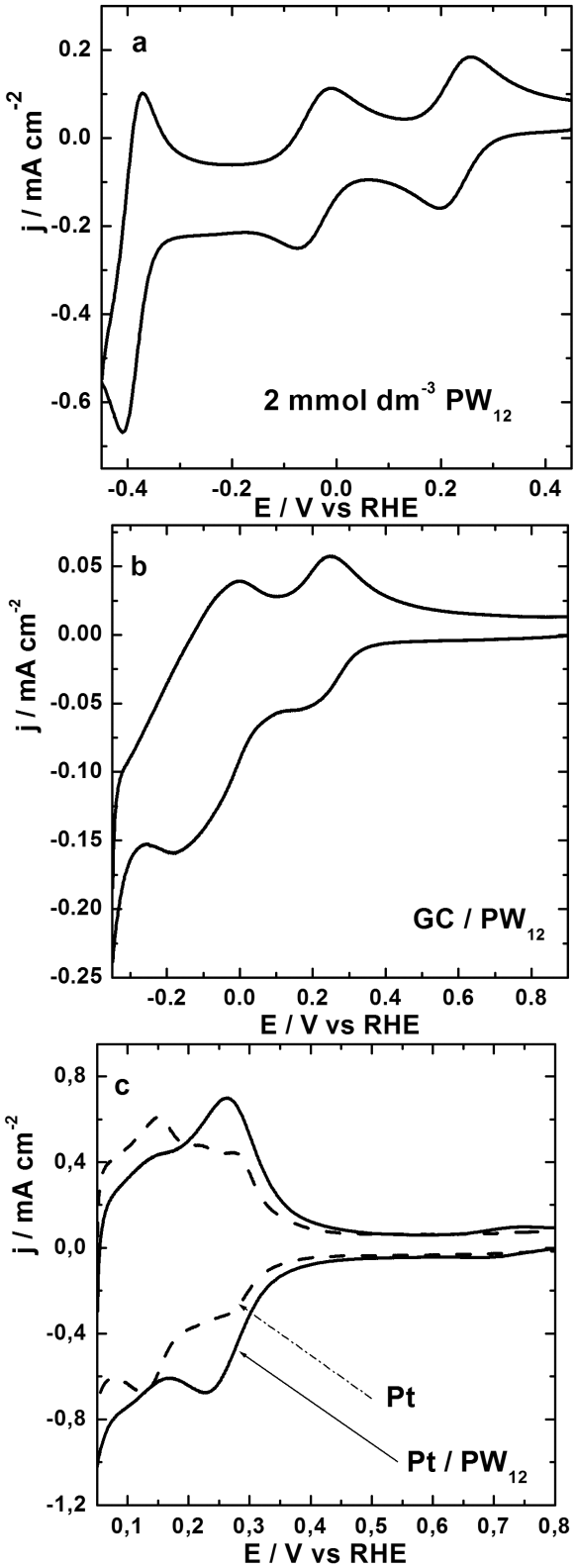

Fig. 1. Cyclic voltammetric responses of (a) 5 mmol dm^{-3} solution of $H_3PW_{12}O_{40}$, and PW_{12} monolayer type adsorbates on (b) glassy carbon (diameter, 3 mm) and (c) platinum (diameter, 2 mm) recorded in 0.5 mol dm^{-3} H_2SO_4 (deoxygenated). Scan rate: 50 mV s^{-1}.

trode was placed in an oven at 60 °C for 1h. Afterwards, the electrode was dipped into 3 mmol dm^{-3} solution of $H_3PW_{12}O_{40}$ (PW_{12}) in water for 15 min. To assemble PW_{12}-stabilized Pt nanoparticles, a glassy carbon electrode was exposed to the solution (colloidal suspension) of PW_{12}-protected platinum (Pt-PW_{12}) particles for 30 min, followed by rinsing with water.

In order to verify the adsorption properties of GC and polycrystalline Pt, parallel experiments were performed using GC (diameter, 3 mm) and Pt (diameter, 2 mm) disk electrodes. Modification of the electrode surfaces with monolayer type adsorbate of PW_{12} was achieved by dipping the electrodes for 8 h in the respective 5 mmol dm^{-3} solution.

In order to form bioelectrocatalytic layer, first 0.5 ml of the aqueous horseradish peroxidase (3.5 mg/ml) had been introduced onto the glassy carbon electrode surface modified with the phosphomolybdade-covered multi-walled carbon nanotubes [18] (fabricated by dropping the respective colloidal suspension stabilized with Nafion). This step was followed by overnight drying, rinsing with water, and subsequent immobilization of 5 µl of 3 mmol dm^{-3} metaloporphyrin solution.

Electrochemical measurements were done with CH Instruments (Austin, U.S.A.) Model 650 workstation. A standard three-electrode cell was used for all experiments. The rotating disk voltammetric measurements were done using the Metrohom rotating disk electrode assembly. A platinum flag was used as the counter electrode. A saturated calomel electrode (SCE) was used as a reference electrode; it was placed in the second compartment and connected to the main cell through a Lugging capillary. All potentials are expressed against the reversible hydrogen electrode (RHE).

3. RESULTS AND DISCUSSION

3.1. Electrocatalytic oxygen reduction in acid medium

Our preliminary voltammetric experiments (Fig. 1) were aimed at providing general information about the nature of redox reactions of $H_3PW_{12}O_{40}$, PW_{12}, in solution (a) and after adsorption on carbon (b) and platinum (c) electrode surfaces. Fig. 1a shows a typical cyclic voltammetric response of the system dissolved in 0.5 mol dm^{-3} H_2SO_4 at 3 mmol level. It is noteworthy that electrochemical properties the PW_{12} are characterized by multi-step electron transfers. The first two, most positive, pro-

cesses are typically one-electron reactions in the case of polytungstates [19].

Another important issue is that heteropolytungstates and heteropolymolybdates undergo irreversible adsorption (or chemisorption) on both carbon and platinum. Figs 1b and 1c illustrate cyclic voltammograms of PW_{12} adsorbed on glassy carbon (GC) and platinum electrodes, respectively, recorded in 0.5 mol dm^{-3} H_2SO_4. For Keggin type polyoxometallates, the monolayer type coverage on both GC and Pt have been postulated [7,16,17]. Due to the appearance of hydrogen adsorption peaks, the existence of surface reactions related to the formation of PtO and the possibility of interference from proton reduction, the phosphotungstate responses are generally better defined when the systems are immobilized on GC rather than Pt substrates.

In the potential range down to 0 V, PW_{12} is characterized by the reversible one-electron process that can be described as follows [16,20]:

$$PW^{VI}_{12}O_{40}^{3-} + e^- \Leftrightarrow PW^{V}W^{VI}_{11}O_{40}^{4-}. \quad (1)$$

The related set of voltammetric peaks at about 0.25 V is overlapping the hydrogen adsorption peaks that typically exist at clean bare Pt (Fig. 1c). The system's (PW_{12}) second one-electron reduction reaction requires simultaneous injection of electron and proton [20] but its appearance on Pt is already complicated by the proton discharge reaction. Polytungstates adsorbed on Pt have been reported to interact with hydrogen adatoms to form mixed hydrogen/tungstate adlayers that are characterized by reversible redox behavior interpreted in terms of spillover effect [16]. The latter phenomenon explains fairly high reduction currents around 0.05-0.1 V, at least relative to what one would expect on bare (unmodified) Pt nanoparticles [17].

It is commonly accepted that, during reductions, introduction of more than 4-6 electrons per heteropolyunit leads to structural reorganization and irreversible redox behavior. It is apparent from Fig. 1b that, when PW_{12} is immobilized on GC, the latter phenomena appear at potentials more negative than -0.3. For Pt surfaces, the practical potential limits are from ca.1.0 to 0.1 V. Thus one can conclude that, in the potential range of interest to the voltammetric (including RDE) investigations of oxygen reduction, PW_{12} adsorbate shall remain stable on Pt and carbon surfaces. It can also be expected that PW_{12} should retain its electroactivity following adsorption on GC and Pt surfaces [16,17].

To get insight into dynamics of the electrocatalytic reduction of oxygen reduction at the

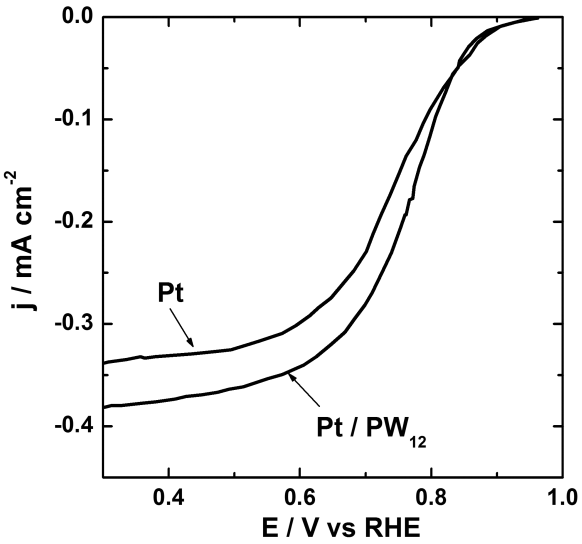

Fig. 2. RDE voltammograms recorded in the oxygen saturated (C_{Ox} = 1.1*10^{-6} mol cm^{-3} [21]) 0.5 mol dm^{-3} H_2SO_4 using GC-supported Pt nanoparticles, bare and modified with PW_{12}. Rotation rate, 1660 rpm. Scan rate, 10 mV s^{-1}. Pt loading, 24 μg cm^{-2}.

carbon supported Pt nanoparticles, bare and modified with PW_{12}, we performed diagnostic rotating disk electrode (RDE) voltammetric measurements. Typical well-defined RDE current - potential curves recorded at 1660 rpm rotation rate in the oxygen saturated (O_2 concentration, ca. 1.1 mmol dm^{-3} [21]) 0.5 mol dm^{-3} H_2SO_4 solution are illustrated in Fig. 2. Here the loading, distribution and morphology of carbon supported Pt nanoparticles were approximately the same. It is noteworthy that current densities were somewhat higher for GC-supported Pt nanoparticles modified with PW_{12} when compared to bare Pt particles. Obviously, the RDE currents of Fig. 2 were under some kinetic control (they were not purely convective-diffusional) with such a low loading of Pt (24 mg cm^{-2}). Further, the result of Fig. 2 implies somewhat more efficient electrocatalysis at platinum modified with PW_{12} at least under conditions of Fig. 2.

We have also performed RDE voltammetric experiments at different rotation rates. The dependence of the respective RDE limiting currents versus the square root of rotation rate (Fig. 3a) shows some deviation from linearity (dotted line), i.e. from the ideal behavior characteristic of a system limited solely by convective diffusion of oxygen in solution, at rotation rates higher than ca. 1000 rpm. This result implies that, only at faster rotation rates,

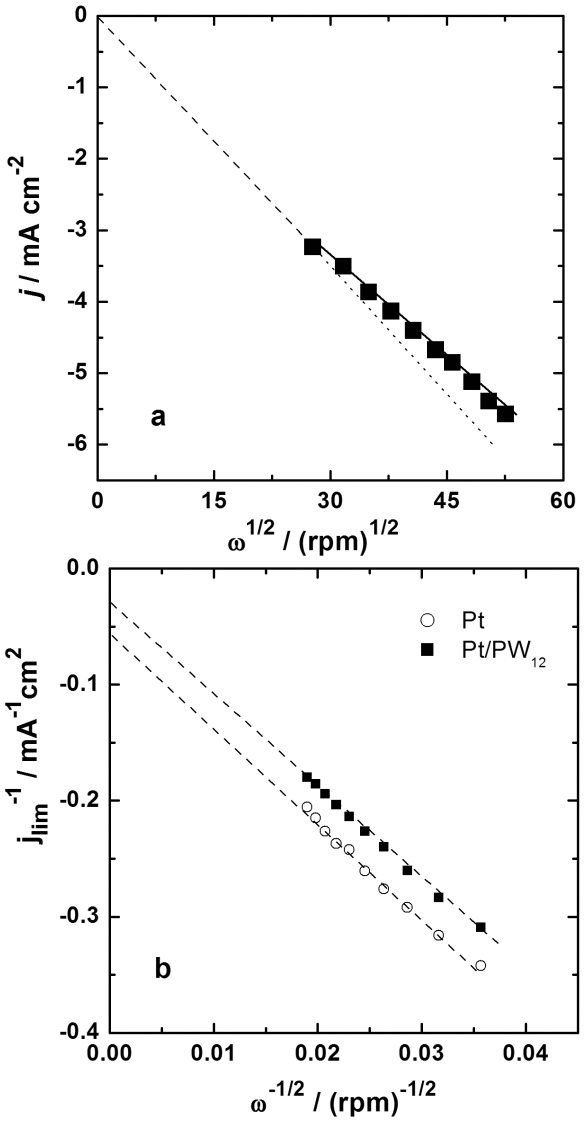

Fig. 3. (a) Dependence of RDE limiting currents (recorded as for Fig. 2 using PW_{12}-modified GC-supported Pt nanoparticles) on the square root of rotation rate; and **(b)** the related Koutecky-Levich plots using currents measured at 0.3 V. For comparison, the analogous plot is provided for bare (unmodified) GC-supported Pt nanoparticles of the same loading (24 μg cm^{-2}).

the electrocatalytic reaction was too slow to allow the convective-diffusional control to be operative. Assuming the approximately first order reaction kinetics [21], the RDE voltammetric limiting current densities (j_{lim}) can be described as reciprocals [22] using the Koutecky-Levich formalism:

$$j_{lim}^{-1} = (nFk\Gamma_{film}C_{Ox})^{-1} + j_{Lev}^{-1}, \qquad (2)$$

where j_{Lev} limiting current density is given by the classic Levich equation (in which the convective diffusion component is proportional to the square root of rotation rate), k is a rate constant for the catalytic chemical reaction at the film/solution interface or within the film (in the homogeneous reaction meaning and units), Γ_{film} is the surface concentration of the catalytic centers in the film, and C_{Ox} is the bulk concentration of oxygen in the electrolyte. The symbols n and F stand for the number of electrons involved in the process and the Faraday constant.

It is noteworthy that the Koutecky-Levich slopes in Fig. 3b are approximately the same for both PW_{12}-modified and bare GC-supported Pt nanoparticles. At potential as low as 0.3 V, platinum exists in its pure metallic form (i.e. where hydrogen adsorption peaks are absent and no platinum oxide is formed yet) and, in view of previous literature reports [21,23-26,35], it is reasonable to expect that n to be equal to 4 for the bare platinum electrocatalyst. The similarity of slopes in Fig. 3b allows us to extend the assumption about involvement of four electrons (implying the ideal reduction mechanism proceeding effectively to water) in the case of PW_{12}-modified GC-supported Pt nanoparticles.

The analysis [21-25] of Koutecky-Levich reciprocal plots (Fig. 3b) yielded for PW_{12}-modified GC-supported Pt nanoparticles a fairly small positive intercept equal to about 0.011 mA^{-1} cm^2. Using the approach described before [22], the kinetic parameter, namely the intrinsic rate constant of heterogeneous charge-transfer - k_{het} (which is equivalent to the product of $k\Gamma_{film}$ in Eq. (2), has been found to be equal to ca. $2.2 \cdot 10^{-1}$ cm s^{-1} for the catalytic electroreduction (in 0.5 mol dm^{-3} H_2SO_4) of oxygen at 0.3 V using the electrode of GC-supported Pt nanoparticles (loading, 24 mg cm^{-2}) modified with PW_{12}. When we have performed the analogous kinetic analysis for the electrode modified with PW_{12}-free Pt nanoparticles (prepared as for the Inset in Fig. 5), the intrinsic rate constant is on the level $1 \cdot 10^{-1}$ cm s^{-1}. In the above considerations, the Koutecky-Levich lines have been analyzed (according to Eq. (2)) with the assumption of first-order reaction kinetics. The unit reaction order was also reported in literature [21,23,24] at different platinum based catalytic surfaces.

We also performed RDE voltammetric measurements (Fig. 4a) to diagnose the oxygen reduction at a glassy carbon electrode modified with PW_{12}-protected Pt nanoparticles (loading, 30 mg cm^{-2}) that had been prepared independently in a

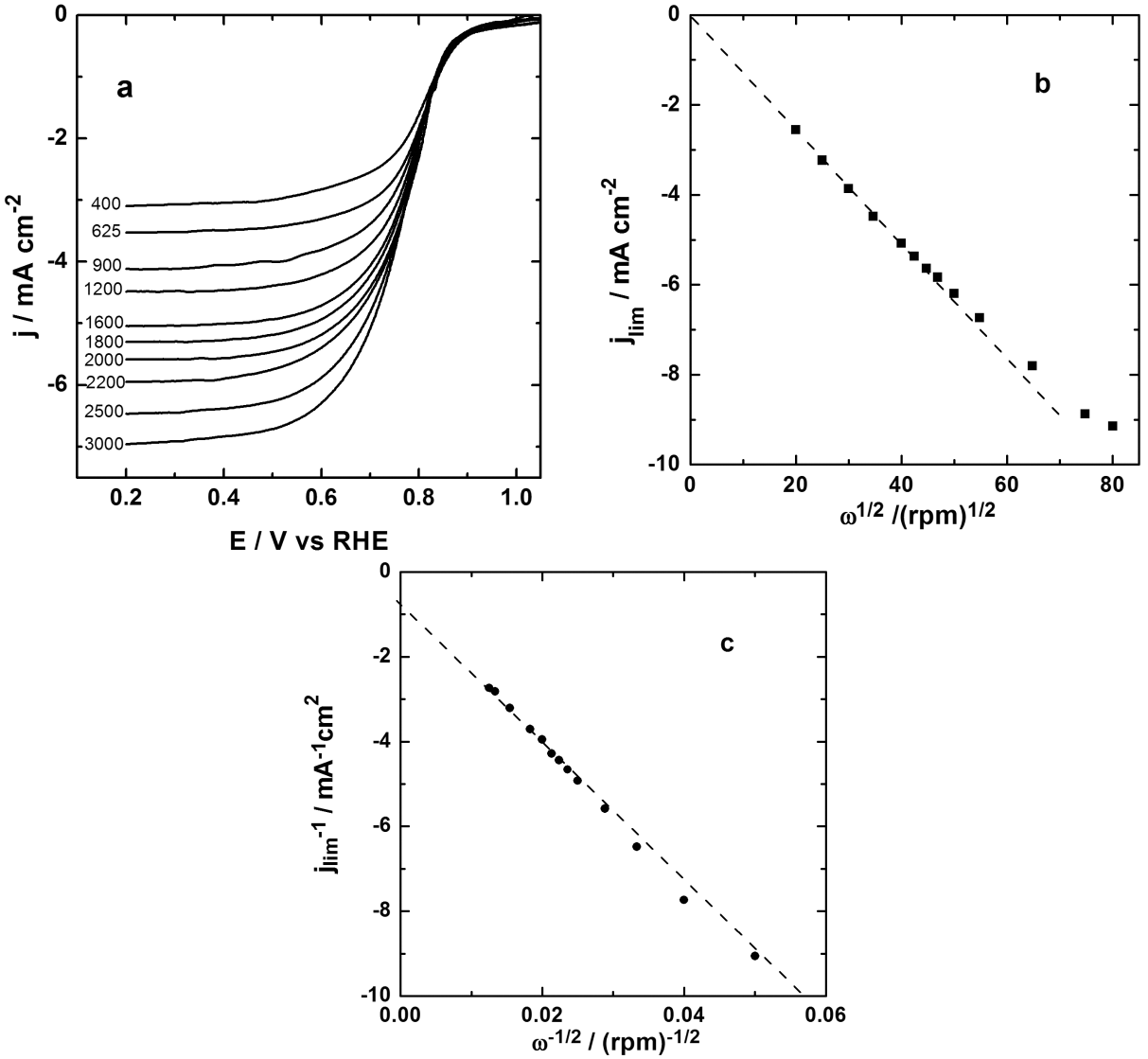

Fig. 4. (a) Representative RDE voltammogram recorded in the oxygen-saturated solution at at different rotation rates (400, 625, 900, 1200, 1600, 1800, 2000, 2200, 2500, 3000 rpm) using PW_{12}-protected Pt nanoparticles. Scan rate, 10 mV s^{-1}. Electrolyte, 0.5 mol dm^{-3} H_2SO_4. **(b)** Dependence of Levich (limiting) currents on square root of rotation rate; and **(c)** the related Koutecky-Levich reciprocal plot. Limiting currents were measured at 0.3 V. Pt loading, 30 μg cm^{-2}.

form of stable colloidal solution. The dependence of the respective RDE limiting currents versus the square root of rotation rate (Fig. 4b) showed, as before (Fig. 3b), the deviation from linearity (dotted line). The analysis, performed by means of so-called Koutecky-Levich reciprocal plots (Fig. 4c) yielded a fairly small positive intercept equal to about 0.04 mA^{-1} cm^2. Thus the kinetic parameter, namely the intrinsic rate constant of heterogeneous charge-transfer, was found to be ca. $5 \cdot 10^{-2}$ cm s^{-1} for the catalytic electroreduction (in 0.5 mol dm^{-3} H_2SO_4) of oxygen at 0.3 V. Since systems of Figs. 3 and 4 differed presumably in the morphology, unequivocal comparison of the respective kinetic results is not possible here. Certainly, stabilizing or modifying Pt nanoparticles with PW_{12} not only does not inhibit but also tends to activate the electroreduction of dioxygen. What is probably even more important, that no ring current (at 1.2 V) was detected, i.e. no hydrogen peroxide intermediate was formed during the RDE measurements with use of PW_{12}-Pt nanoparticles. The latter result im-

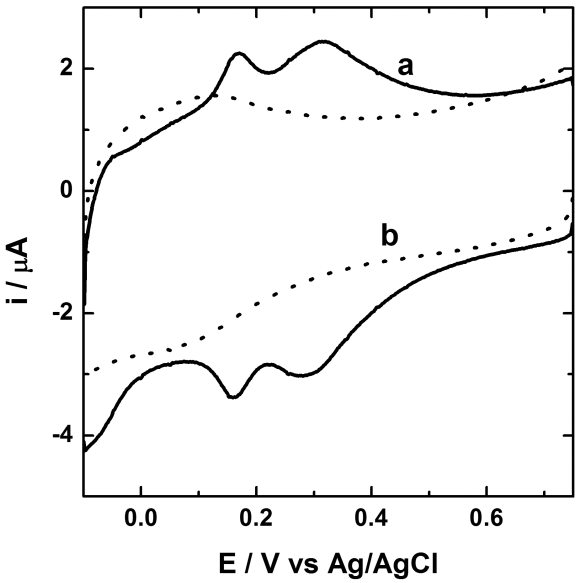

Fig. 5. Cyclic voltammetric responses of phoshomolybdate-modified carbon nanotubes (immobilized on glassy carbon) recorded in (a) 0.5 mol dm^{-3} H_2SO_4, and (b) 0.1 mol dm^{-3} KCl. Scan rate, 50 mV s^{-1}.

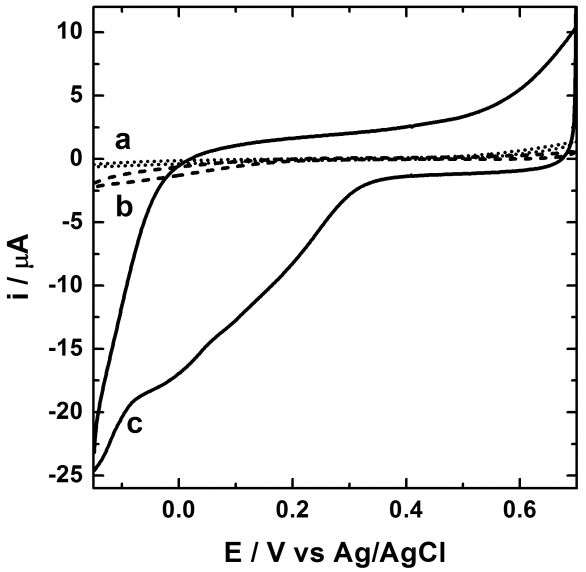

Fig. 6. Voltammetric reduction of oxygen at glassy carbon electrode covered with Co-porphirin (curve *b*) and phoshomolybdate-modified carbon-nanotube-supported horseradish peroxidase together with Co-porphirin (curve *c*). Curve *a* describes the background response of the Co-porphyrin covered electrode in the absence of oxygen. Loading of Co-porphyrin, $2.1 \cdot 10^{-7}$ mol cm^{-2}. Electrolyte: argon or oxygen saturated 0.1 mol dm^{-3} KCl. Scan rate, 5 mV s^{-1}.

plies the effectively four-electron electroreduction of oxygen (to water) under conditions of the Fig. 4 experiment.

3.2. Bioelectrocatalytic hybrid system for oxygen reduction

Electrocatalytic systems that would be useful in biological media or the systems utilizing biocatalysts (enzymes) have to operate in neutral solutions. Unless highly specific and expensive enzymes, such as bilirubin oxidase or laccase, are considered [27-33], the reduction of oxygen in neutral media is a two-step process suffering from the formation of hydrogen peroxide as undesirable intermediate product. Therefore our bioelectrocatalytic system is composed of two components: the macromolecular metalloporphyrine centers capable of initiating the reduction of oxygen (mostly to hydrogen peroxide) and the enzymatic part (horseradish peroxidase) that is highly reactive towards electrocatalytic decomposition of hydrogen peroxide intermediate to water as a final product. As conductive and robust supports, we also utilize the recently proposed by us the polyoxometallate ($PMo_{12}O_{40}^{3-}$) modified multi-walled carbon nanotubes [18]. Such heteropolymolybdate derivatized carbon nanostructures are likely not only to facilitate the overall charge distribution to catalytic (metaloporphyrin and enzymatic) sites but also to stabilize the hybrid (composite) film by interacting with positively charged portions of the enzyme and Co-protoporphyrine sites. Fig. 5 shows the responses of $PMo_{12}O_{40}^{3-}$-modified carbon nanotubes (immobilized on glassy carbon simply by dip coating in manner described elsewhere [18]) in (a) acid solution and (b) more neutral medium. An important issue is that, despite change of pH, $PMo_{12}O_{40}^{3-}$-modified carbon nanotubes retain their interfacial electroactivity and stability. The pH increase seems to result in overlapping of two-electron phosphomolybdate redox transitions [18]. The presence of negatively charged polyanion is likely facilitate attachment (via electrostatic interaction with positively charged portions) of Co-protoporphyrin and the horseradish peroxidase.

The presence of carbon nanotubes and the enzyme has also activating effect on the Co-porphyrin-catalyzed oxygen reduction. While curves *a* and *b* in Fig. 6 show the responses of the conventional porphyrin layer on glassy carbon in the

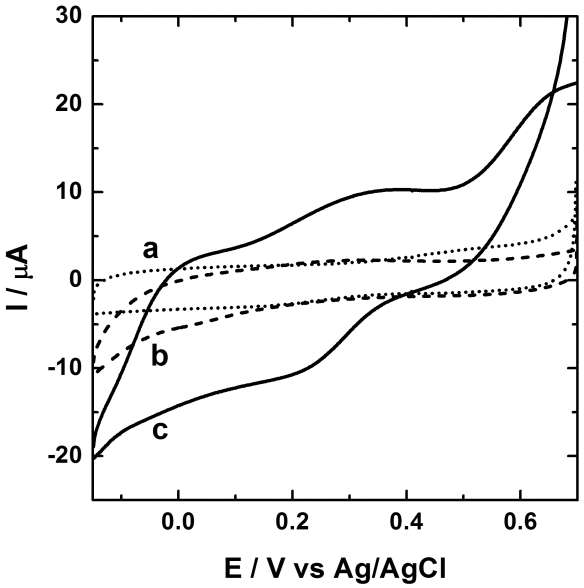

Fig. 7. Voltammetric reduction of hydrogen peroxide (5 mmol dm^{-3}) at glassy carbon electrode covered with phoshomolybdate-modified carbon-nanotube-supported horseradish peroxidase with (curve *c*) and without (curve *b*) Co-porphirin. Curve *a* describes the background response of the electrode covered with phoshomolybdate-modified carbon-nanotube-supported horseradish peroxidase in the absence of oxygen. Other parameters as for Fig. 6.

absence and presence of oxygen, curve *c* in Fig. 6 refers to the oxygen reduction at the film of phosphomolybdate-modified carbon- nanotube-supported horseradish peroxidase together with Co-porphyrin. First, the voltammetric reduction of oxygen at the composite film (curve *c*) appears at more positive potential (relative to curve *b*). Further, the reduction currents are more than order of magnitude higher in the case of curve *c* in comparison with curve *b*. The overall enhancement effect should be attributed to the improved distribution of charge (due to the presence of highly-conducting multi-walled carbon nanotubes) and the bifunctional nature of the metalloporphyrin/enzyme bioelectrocatalytic system capable of inducing electroreduction of both oxygen and undesirable hydrogen peroxide intermediate. Indeed, it is apparent form the data of Fig. 7 that carbon-nanotube-supported horseradish peroxidase (particularly containing immobilized metalloporphirin) exhibits sizeable electrocatalytic reactivity towards reduction of H_2O_2 in neutral medium. Judging from curve *c* (Fig. 7), it is reasonable to expect that most of hydrogen peroxide produced during electroreduction of oxygen at the hybrid (composite) bioelectrocatalyst (Fig. 6, curve *c*) is reductively decomposed to water at the approximately the same potentials where oxygen is reduced (Compare curves *c* in Figs. 6 and 7). Consequently, the overall oxygen reduction mechanism of Fig. 6c is likely to be closer to the 4-electron one (reduction to water) rather than the 2-electron one (reduction to hydrogen peroxide). To confirm this hypothesis, further research is still necessary along this line.

4. CONCLUSIONS

Both modification of GC-supported platinum nanoparticles with PW_{12} and utilization of PW_{12}-protected (or stabilized) Pt nanoparticles (immobilized on GC) produce highly reactive platinum-based centers towards reduction of oxygen. Like in the case of bare platinum, the overall reduction mechanism is unchanged and it seems to involve effectively four electrons producing directly water as a final product. Having in mind the chemical analogies between PW_{12} and tungsten oxide, it is likely that PW_{12} provides similar environment to tungsten oxide/hydrogen bronzes [22,34]. The important issues are the ability of PW_{12} to form strong electroactive adsorbates on solid surfaces, its high reductive reactivity and fast electron transfer (mediating) capabilities, as well as its super-acid characteristics leading to the increased availability and mobility of interfacial protons. When combined with the specific reactivity of Pt inducing the reduction of oxygen, the above properties should promote a bifunctional electrocatalytic mechanism in which PW_{12} facilitates decomposition of the undesirable hydrogen peroxide intermediate. Our results are also consistent with the view that chemisorption of PW_{12} must have not blocked appreciably active sites of catalytic Pt.

When it comes to the bioelectrocatalytic reduction of oxygen in neutral medium, high reductive reactivity of horseradish peroxidase towards hydrogen peroxide and fast electron electron distribution capabilities of carbon nanotubes make the composite system very attractive in the application as matrix for the Co-porphyrin catalytic centers. While the electrocatalytic reduction of oxygen is initiated at metaloporphyrin sites, the carbon-nanotube-supported enzyme facilitates decomposition of the undesirable hydrogen peroxide intermediate and makes the overall reduction effectively closer to the 4-electron process.

ACKNOWLEDGEMENTS

The support from Ministry of Science and Information Technology (Poland) under the State Committee for Scientific Research (KBN) grant N20416432 /4284 and project PBZ 18-KBN098/T09/2003 is highly appreciated. Partial support from the Network Efficient Oxygen Reduction for Electrochemical Energy Conversion (coordinated by ZSW, Ulm, Germany) is also acknowledged. This work was also funded by Ministero dell'Istruzione dell'Università e della Ricerca (MIUR), Italy under the project FISR 2001. R. W. and A. K.-Z. thank the University of Camerino for supporting their stays in Camerino.

REFERENCES

[1] B. Keita, L. Nadjo and J. Haeussler // *J. Electroanal. Chem.* **243** (1988) 481.
[2] B. Wang and S. Dong // *Electrochim. Acta* **41** (1996) 895.
[3] S. Dong and Z. Jin // *J. Chem. Soc. Chem. Commun.* (1987) 1871.
[4] X. Xi and S. Dong // *Electrochim. Acta* **40** (1995) 2785.
[5] B. Keita, A. Belhouori and L. Nadjo // *J. Electroanal. Chem.* **314** (1991) 345.
[6] B. Keita and L. Nadjo // *J. Electroanal. Chem.* **240** (1988) 325.
[7] D. Ingersoll, P.J. Kulesza and L.R. Faulkner // *J. Electrochem. Soc.* **141** (1994) 140.
[8] L. Adamczyk, P.J. Kulesza, K. Miecznikowski, B. Palys, M. Chojak and D. Krawczyk // *J. Electrochem. Soc.* **152** (2005) E98.
[9] K.K. Kasem and F.A. Schultz // *Can. J. Chem.* **73** (1995) 87.
[10] Y. Izumi and K. Urabe // *Chem. Lett.* **20** (1991) 663.
[11] R.F. Service // *Science* **305** (2004) 1225.
[12] J.A. Poirier and G. Stoner // *J. Electrochem. Soc.* **141** (1994) 425.
[13] E.A. Ticianelli, C.R. Derouin, A. Redondo and S. Srinivasan // *J. Electrochem. Soc.* **185** (1988) 2209.
[14] O. Savadogo and K.C. Mandal // *J. Electrochem. Soc.* **139** (1992) L16.
[15] M. Chojak, M. Mascetti, R. Wlodarczyk, R. Marassi, K. Karnicka, K. Miecznikowski and P.J. Kulesza // *J. Solid State Electrochem.* **8** (2004) 854.
[16] M. Borzenko, M. Chojak, P.J. Kulesza, G.A. Tsirlina and O.A. Petrii // *Electrochim. Acta* **48** (2003) 3797.
[17] P.J. Kulesza, M. Chojak, K. Karnicka, K. Miecznikowski, B. Palys, A Lewera and A. Wieckowski // *Chem. Mater.* **16** (2004) 4128.
[18] P.J. Kulesza, M. Skunik, B. Baranowska, K. Miecznikowski, M. Chojak, K. Karnicka, E. Frackowiak, F. Beguin, A. Kuhn, M.-H. Delville, B. Starobrzynska and A. Ernst // *Electrochim. Acta* **51** (2006) 2373.
[19] A. Lewera, M. Chojak, K. Miecznikowski and P.J. Kulesza // *Electroanalysis* **17** (2005)1471.
[20] Kulesza, K. Karnicka, K. Miecznikowski, M. Chojak, A. Kolary, P.J. Barczuk, G. Tsirlina and W. Czerwinski // *Electrochim. Acta* **50** (2005) 5155.
[21] Zacevic, J.S. Wainright, M.H. Litt, S.Lj. Gojkovic and R.F. Savinell // *J. Electrochem. Soc.* **144** (1997) 2973.
[22] P.J. Kulesza, B. Grzybowska, M.A. Malik and M.T. Galkowski // *J.Electrochem. Soc.* **144** (1997) 1911.
[23] Markovic, R.R. Adzic, C.D. Cahan and E.B. Yeager // *J. Electroanal. Chem.* **377** (1994) 24.
[24] D.B. Sepa, M.V. Vojnovic, Lj.M. Vracar and A. Damjanovic // *Electrochim. Acta* **32** (1987) 129.
[25] F. Maillard, M. Martin, F. Gloaguen and J.-M. Leger // *Electrochim. Acta* **47** (2002) 3431.
[26] J. Jiang and B. Yi // *J. Electroanal. Chem.* **577** (2005) 107.
[27] N. Mano, H-H. Kim, Y. Zhang and A. Heller // *J. Am. Chem. Soc.* **124** (2002) 6480.
[28] S.C. Barton, H-H. Kim, G. Binyamin, Y. Zhang and A. Heller // *J. Phys. Chem. B* **105** (2001) 11917.
[29] S. Tsujimura, M. Kawaharada, T. Nakagawa, K. Kano and T. Ikeda // *Elecrochem. Commun.* **5** (2003) 138.
[30] S. Tsujimura, H. Tatsumi, J. Ogawa, S. Shimizu, K. Kano and T. Ikeda // *J. Electroanal. Chem.* **496** (2001) 69.
[31] F. Barriere, Y. Ferry, D. Rochefort and D. Leech // *Elecrochem. Commun.* **6** (2004) 237.
[32] S. Shleev, A. El Kasmi, T. Ruzgas and L. Gorton // *Elecrochem. Commun.* **6** (2004) 934.
[33] G. T. Palmore and Hyug-Han Kim // *J. Electroanal. Chem.* **464** (1999) 110.
[34] P.J. Kulesza and L.R. Faulkner // *J. Electroanal. Chem.* **259** (1989) 81.
[35] K.E. Gubbins and R.D. Walker // *J. Electrochem. Soc.* **112** (1965) 469.